LETTER

doi:10.1038/nature23483

New evidence for mammaliaform ear evolution and feeding adaptation in a Jurassic ecosystem

Zhe-Xi Luo[1,2], Qing-Jin Meng[3], David M. Grossnickle[2], Di Liu[3], April I. Neander[1], Yu-Guang Zhang[3] & Qiang Ji[4]

Stem mammaliaforms are forerunners to modern mammals[1], and they achieved considerable ecomorphological diversity in their own right[2]. Recent discoveries suggest that eleutherodontids, a subclade of Haramiyida, were more species-rich during the Jurassic period in Asia than previously recognized[3–12]. Here we report a new Jurassic eleutherodontid mammaliaform with an unusual mosaic of highly specialized characteristics[1–6], and the results of phylogenetic analyses that support the hypothesis that haramiyidans are stem mammaliaforms. The new fossil shows fossilized skin membranes that are interpreted to be for gliding and a mandibular middle ear with a unique character combination previously unknown in mammaliaforms. Incisor replacement is prolonged until well after molars are fully erupted, a timing pattern unique to most other mammaliaforms. *In situ* molar occlusion and a functional analysis reveal a new mode of dental occlusion: dual mortar–pestle occlusion of opposing upper and lower molars, probably for dual crushing and grinding. This suggests that eleutherodontids are herbivorous, and probably specialized for granivory or feeding on soft plant tissues. The inferred dietary adaptation of eleutherodontid gliders represents a remarkable evolutionary convergence with herbivorous gliders in Theria. These Jurassic fossils represent volant, herbivorous stem mammaliaforms associated with pre-angiosperm plants that appear long before the later, iterative associations between angiosperm plants and volant herbivores in various therian clades.

Clade Mammaliaformes[1]
Clade Haramiyida (emended by ref. 11)
Family Eleutherodontidae[4,11]
Vilevolodon diplomylos gen. et sp. nov.

Etymology. *Vilevol* (Latin): glider; *don* (Greek): tooth, and a common suffix for mammalian taxon names; *diplo* (Greek): double; *mylos* (Greek): grinding; *diplomylos* refers to the dual mortar–pestle occlusion of opposing upper and lower molars.

Holotype. Beijing Museum of Natural History PM002942A and B (abbreviated as BMNH2942A and BMNH2942B) are the main slab and counter slab, respectively, preserved with carbonized residues of patagial skin membranes associated with a postcranial skeleton that is 70% complete. The skull is preserved with teeth in occlusion and a middle ear associated with the mandible (Figs 1, 2, Extended Data Figs 1–3).

Geological age. *Vilevolodon diplomylos* type specimen is from the Nanshimen site of the Tiaojishan Formation in Qinglong County, Hebei Province, China, stratigraphically correlated by the regional index fossil *Qaidamestheria*[13], and estimated to be 161–160 million years old. The Tiaojishan Formation has yielded additional mammaliaforms at the same site and elsewhere[9–11,14–16].

Diagnosis. Among haramiyidans, *Vilevolodon* is most similar to *Arboroharamiya*[10] and *Xianshou*[11] in having dual mortar–pestle molar occlusion in which the tallest distal cusp A^1 of the upper molar (upper 'pestle') occludes into the distal basin (lower 'mortar') of the opposite lower molar. The tallest mesial cusp A_1 of the lower molar (lower pestle) occludes into the mesial basin (upper mortar) of the opposite upper molar (Figs 1, 2, Extended Data Figs 3–6; Supplementary Video 1). It differs from *Maiopatagium*[15] and *Shenshou*[11] in that upper molars are arranged in successively imbricated series in which M^2 is oblique to M^1, and M^1 is oblique to P^4. This is mirrored by imbrication of the lower teeth in which M_2 is medial (and oblique) to M_1, and M_1 is medial to P_4 (Fig. 1). This differs from the straight tooth rows of *Maiopatagium* and *Shenshou* (Fig. 2). Among eleutherodontids (see Supplementary Information), *V. diplomylos* is most similar to species of *Xianshou* in having a hypertrophied P^4 and pronounced flexure of upper P^3–P^4 that is correlated with rostroventral bending of the maxilla. Differs from *Xianshou* species in having larger teeth but a shorter mandible. Differs from paulchoffatiid multituberculates[16] in that its molars have a confluent root in a single alveolus, not double roots in separate alveoli. Differs from eutriconodonts and spalacotherioids of crown mammals in that Meckel's sulcus is vestigial and Meckel's element is shortened[17,18]. Full differential diagnosis of *V. diplomylos* from other mammaliaforms is provided in the Supplementary Information.

The unique dental occlusion of *Vilevolodon* includes dual crushing and grinding functions. Our simulation analysis using STL models from computed tomography scans shows evidence of complex chewing movement in two separate occlusal cycles (Supplementary Video 1 and Extended Data Fig. 6). The trenchant cusp of P_4 contacts the P^4 basin simultaneously with the dual mortar–pestle occlusion of M^1/M_1 and M^2/M_2 in the same chewing cycle (Supplementary Video 1 and Extended Data Fig. 6). The main trajectory of cusp A_1 (pestle) of the lower molar is ortho-palinal, similar to that of *Haramiyavia*[4,6], but the palinal movement has a strong ventral vector, as constrained by the deep basins of upper and lower molars. It is not possible for the lower P_4–M_2 to move posteriorly and horizontally (that is, fully palinal). This differs from multituberculates, *Megaconus* and *Maiopatagium*, in which the lower teeth can have full palinal movement[4,9,19] (Fig. 2). The dual mortar–pestle occlusal contact and two distinctive occlusal cycles are unique to eleutherodontids (probably also applicable to *Arboroharamiya*), but absent in *Haramiyavia*, *Megaconus*, *Maiopatagium* and other stem mammaliaforms.

We infer that *Vilevolodon* had an herbivorous or omnivorous diet consisting largely of seeds and soft plant parts. Tooth crown complexity of *Vilevolodon* and *Xianshou* is comparable to derived multituberculates with plant-dominated diets[20]. Their tooth crenulations and creases resemble those of sciurid rodents that have diets of nuts, seeds, fruits and young leaves, supplemented by insects[21]. *Vilevolodon* was not a folivore, as it lacks strong tooth crests that are characteristic of primarily folivorous and volant taxa such as dermopterans, anomalurids and marsupial gliders. All modern mammalian gliders are primarily herbivorous and none are primarily insectivorous[22], and we interpret *Vilevolodon* to be a glider based on the presence of carbonized patagia and skeletal morphometric analyses[15]. Thus, our herbivorous dietary inference for *Vilevolodon* is consistent with modern, analogous gliders.

[1]Department of Organismal Biology and Anatomy, The University of Chicago, Chicago, Illinois 60637, USA. [2]Committee on Evolutionary Biology, The University of Chicago, Chicago, Illinois 60637, USA. [3]Beijing Museum of Natural History, Beijing 100050, China. [4]Hebei GEO University, Shijiazhuang 050031, Hebei Province, China.

© 2017 Macmillan Publishers Limited, part of Springer Nature. All rights reserved.

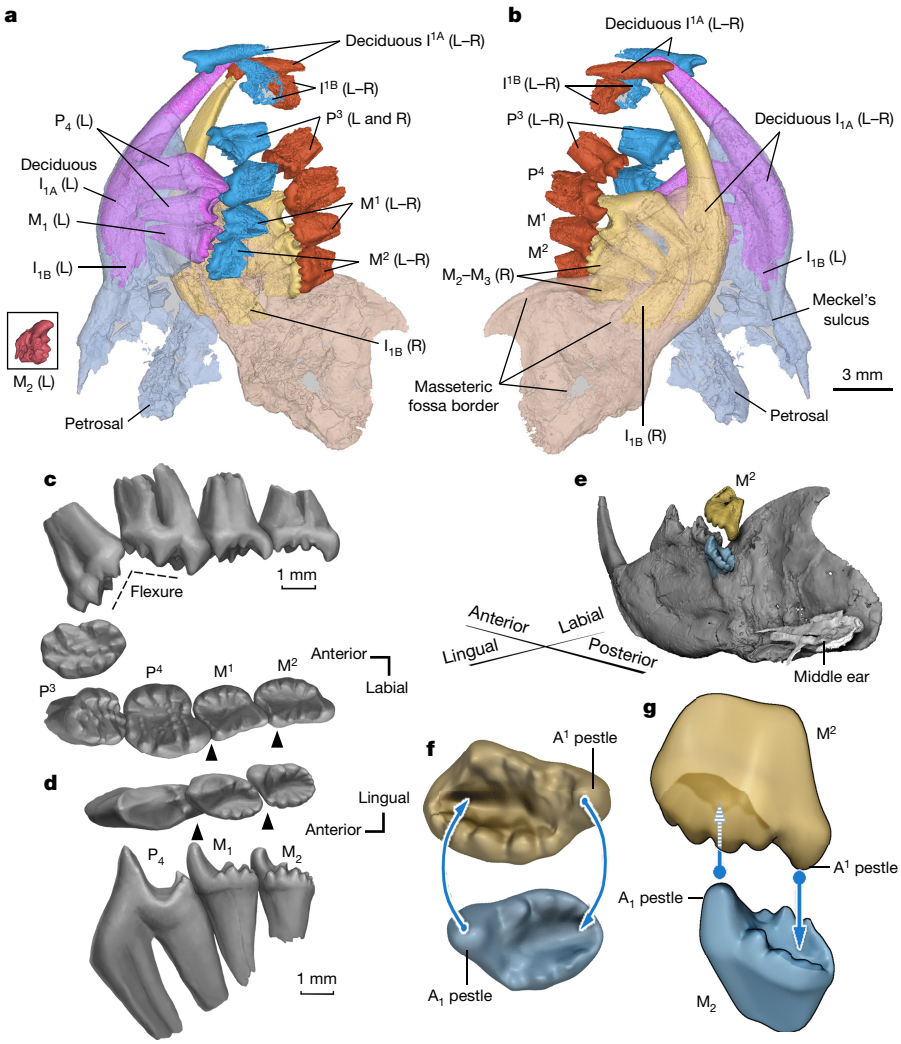

Figure 1 | Dentition of mammaliaform *Vilevolodon diplomylos* (Haramiyida, Eleutherodontidae) (BMNH2942 holotype). **a**, **b**, Mandibles and teeth on BMNH2942A from computed tomography scans (top and under sides); lower M_2 (inset) from BMNH2042B. **c**, Upper teeth in lingual and occlusal views. **d**, Lower teeth in lingual and occlusal views. **e**, Posteromedial view of the mandible to demonstrate the M^2/M_2 occlusal alignment and the middle ear contact to mandible. **f**, Dual mortar–pestle occlusion. The tallest cusp 'A_1 pestle' of lower M_2 occludes into the anterior fusiform mortar basin of M^2 while the tallest cusp 'A^1 pestle' of upper M^2 occludes into the posterior fusiform mortar basin of lower M^2. **g**, M^2/M_2 dual mortar–pestle occlusion in posteromedial view as in **e**. L, left; R, right; P, premolars; M, molars. Lower incisors I_{1A} and I_{1B} are two successive incisor generations of lower locus 1; incisors I^{1A} and I^{1B} are two generations at upper incisor 1 locus. The whole slab and counter-slab with carbonized patagia are shown in Extended Data Fig. 1.

The peculiar teeth of *Vilevolodon* expand the known dental morphological disparity of mammaliaforms. Its densely ornamented and partly basined teeth are markedly distinct from the simplified teeth of *Maiopatagium* and from the straight cusp rows and straight furrow of *Megaconus*. Jurassic eleutherodontids are highly transformed, even compared to Triassic haramiyids of the same clade (Fig. 2). Their disparate tooth morphologies suggest resource partitioning among omnivorous and herbivorous feeding guilds of eleutherodonts. Furthermore, eleutherodonts diversified contemporaneously with early multituberculates[16] and ecomorphologically diverse docodonts[14,23], offering compelling evidence that clade divergence and ecological diversification are coupled in adaptive diversifications in multiple Mesozoic mammaliaform clades[9–11] (Fig. 2).

Eleutherodonts diversified in a pre-angiosperm biota of the Middle to Late Jurassic. Their diets would probably have included seeds, reproductive parts such as strobili and cones of ferns, plus soft meristem tissues and young leaves of seed and gymnosperm plants, which have all been hypothesized to be probable dietary sources for animals[24]. The association of herbivorous and volant eleutherodonts with pre-angiosperm plants in the Jurassic is analogous to the association of herbivorous volant therians (that is, dermopterans, and multiple clades of rodents and marsupials) with angiosperm plants of the Cenozoic era. Eleutherodontids show a marked similarity to the primate *Daubentonia* in the ventrally bent rostrum and deep mandible, and both features are interpreted to be reinforcement for incisor gnawing[25] (Extended Data Fig. 7). *Daubentonia* has a dietary mixture of fruits, exudates and insect larvae. Eleutherodonts and *Megaconus* (Extended Data Fig. 6) show a zigzag tooth row profile in lateral view, convergent with that of frugivorous bats[26] (Extended Data Fig. 7). The highly ornamented teeth of eleutherodontids (*Eleutherodon*, *Sineleutherus*, *Arboroharamiya*, *Xianshou* and *Vilevolodon*) are convergent with some extant sciurid rodents with granivorous and frugivorous diets and to herbivorous phyllostomid bats[21,26]. These observations suggest that haramiyidans differentiated into several feeding guilds during their evolutionary diversification in the Jurassic.

Computed tomography scans of the *Vilevolodon* holotype confirm that premolar loci have no replacing tooth. The right M^2/M_2 are fully erupted and occluded, and these have closed root tips. M^1/M_1 show occlusal wear (Extended Data Fig. 4). Cheek teeth of the *Vilevolodon* have attained adult status[27] according to the individual dental age system detailed in ref. 28. However, its upper and lower incisors are still undergoing replacement, either by a prolonged, or a delayed replacement. Thus, *Vilevolodon* shows a heterochronical pattern of incisor replacement versus premolar and molar eruption, which is unique in mammaliaforms (except *Sinoconodon*)[27]. Either *Vilevolodon* had an unusually accelerated completion of molar eruptions as a juvenile (indicated by ongoing incisor replacement) or the ongoing incisor replacements at I^1/I_1 loci are a paedomorphic adult feature (indicated by complete molar eruption). By contrast, *Morganucodon* and docodontans have modern-mammal-like diphyodont replacements in which replacement of antemolars is completed during juvenile growth stages, well before complete eruption of adult molars[23,29]. This suggests that diphyodont tooth replacement, a hallmark feature for determinate skull growth of modern mammals[27,29], had heterochronical variation, and may be homoplastic in early mammaliaform lineages.

© 2017 Macmillan Publishers Limited, part of Springer Nature. All rights reserved.

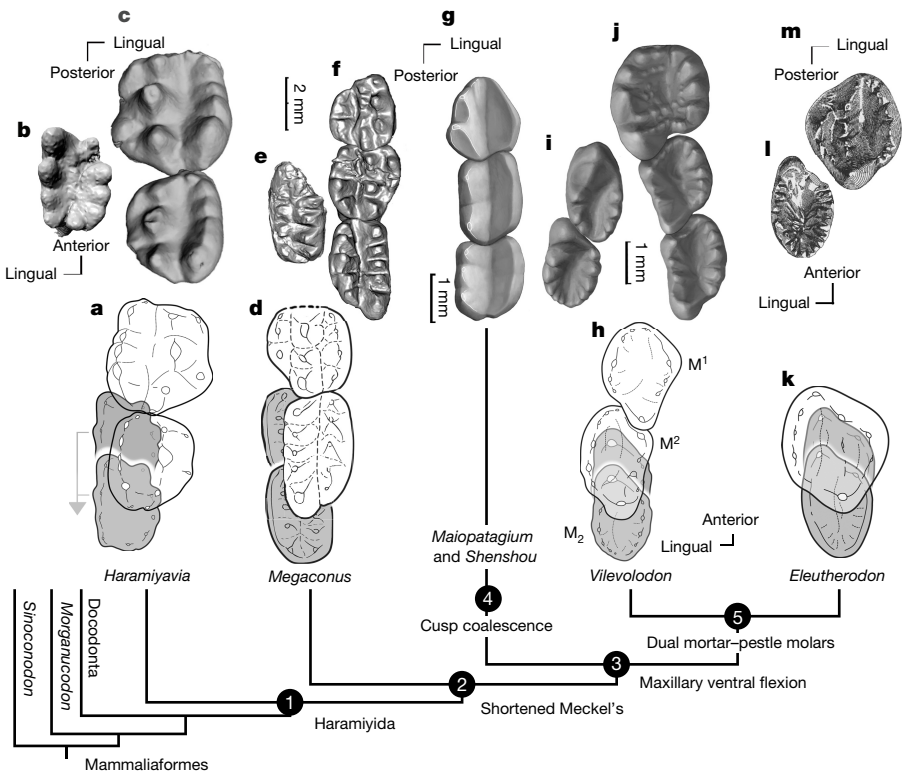

Figure 2 | Disparate tooth occlusal patterns in haramiyidans. a, *Haramiyavia* with lower A_1 of M_3 occluding into lingual embrasure of upper M^2–M^3. Upper tooth outlines flipped and superimposed on lower molar M_3 (ref. 6). **b**, Occlusal view of right M_3. **c**, Occlusal view of right upper M^2–M^3. **d**, *Megaconus*. Lower M_3 A_1 cusp occludes into the lingual embrasure between upper M^2–M^3. **e**, **f**, Right M_3 occlusal view (**e**) and right M^1–M^3 occlusal view (**f**). **g**, *Maiopatagium* right upper P^3–M^2 in occlusal view. **h**–**j**, *Vilevolodon* right lower M_1–M_2 (**i**) and right upper P^4–M^2 (**j**). The opposite upper molars (transparent) over the lower molars (grey) in dual mortar-pestle occlusion. **k**–**m**, *Eleutherodon* putative right M_2 (**l**) and right M^2 (**m**)[3,9]. M^2 (transparent) over M^2 (grey)[3,4]. Node 1, ancestral occlusal pattern of the haramiyidan *Haramiyavia*: thoroughfare occlusal furrow for ortho-palinal occlusal movement. Node 2, clade of *Megaconus* and *Vilevolodon*: shortened Meckel's sulcus and reduced postdentary trough. Node 3, ventro-flexed rostrum. Node 4, cusp coalescence within cusp row, thoroughfare occlusal furrow for ortho-palinal occlusal movement. Node 5, clade of *Vilevolodon* and *Eleutherodon* (including *Xianshou*, *Arboroharamiya* and *Sineleutherus*) with dual mortar–pestle occlusion. Phylogenetic analyses presented in Supplementary Information.

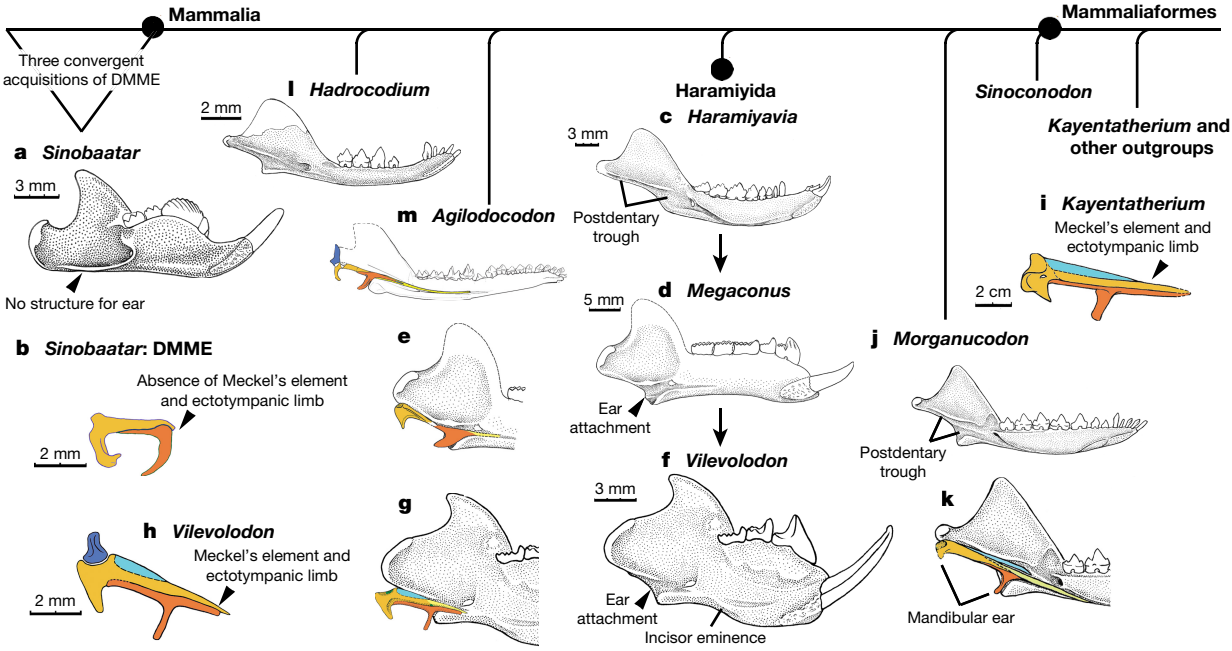

Figure 3 | Transformations of mandibular and middle ear structures among mammaliaforms. a, **b**, Multituberculate *Sinobaatar* mandible (**a**) and middle ear (**b**). The Meckel's element and the anterior limb of ectotympanic are absent from the middle ear, and the mandible has no structure for middle ear connection (BMNH1145 and other specimens). This represents one of at least three evolutionarily independent ear–jaw disconnections in crown mammals. DMME, definitive mammalian middle ear. **c**, *Haramiyavia*[6] mandible. **d**, **e**, Haramiyidan *Megaconus* mandible (**d**) and middle ear (**e**)[9]. **f**–**h**, *Vilevolodon* middle ear removed from right mandible to show attachment structure (**f**); the middle ear restored as on the mandible (**g**); and the middle ear reconstruction showing Meckel's element continuing with the malleus and the ectotympanic with an anterior limb (**h**). Details of fossil and comparison are provided in Extended Data Figs 2, 8 and 9. **i**, The cynodont *Kayentatherium*[30], showing morphological similarities to *Vilevolodon*. **j**–**m**, Mammaliaforms *Morganucodon* (**j**, **k**) *Hadrocodium* (**l**) and *Agilodocodon* (**m**), and their mandibular structure for middle ear attachment. The haramiyidan clade (**c**–**h**) represents an independent evolution in the size reduction of Meckel's element and shortening of the anterior ectotympanic limb, but these are still attached to a vestigial Meckel's sulcus and a reduced postdentary trough. *Vilevolodon* resembles *Kayentatherium* (**i**) and other mammaliaforms but differs from multituberculates with regards to the middle ear (**a**, **b**, **f**–**h**) (see also Extended Data Figs 2, 8 and 9).

© 2017 Macmillan Publishers Limited, part of Springer Nature. All rights reserved.

In *Vilevolodon* the malleus is anteriorly connected to a short ossified Meckel's cartilage (as in refs 17, 18) (which could be interpreted to be the prearticular bone; see Supplementary Information). The ectotympanic (homologous to the angular bone of non-mammalian cynodonts) has an anterior limb and a straight reflected lamina (Fig. 3 and Extended Data Figs 8 and 9). These ear structures are notably similar to those of tritylodontid cynodonts[30]. The anterior limb of the ectotympanic and short Meckel's element are nestled in a triangular depression between the inflected angular process and vertical plate of the mandible. The homologous part of the postdentary trough in the mandibular angle in eleutherodonts represents only a small, reduced part of the full postdentary trough in *Haramiyavia* and other mammaliaforms (Fig. 3 and Extended Data Fig. 9). We confirm that eleutherodonts lack the anterior section of Meckel's sulcus along the ventral margin of the mandible (beyond the mandibular foramen), as noted in earlier studies[11,12]. Meckel's cartilage is much smaller in eleutherodonts than in eutriconodonts and spalacotherioids. We infer that the middle ear would be nestled in the inflected mandibular angle (Extended Data Fig. 9). *Vilevolodon* differs from multituberculates in that multituberculates completely lost the anterior limb of the ectotympanic and the Meckel's element (Fig. 3).

In the phylogenetic context that haramiyidans (including eleutherodontids) are a clade of stem mammaliaforms that exclude multituberculates[1,5,6,15], the shortened Meckel's element and reduced postdentary trough are separately derived features among haramiyidans, as the Late Triassic *Haramiyavia* and other mammaliaforms have a full Meckel's sulcus and postdentary trough (Fig. 3). Size decrease of the middle ear among haramiyidans is convergent with the multiple evolutions of size reduction in crown mammal clades, except that the ear elements had not achieved full separation from the mandible in a dead-end side-branch lineage of mammaliaforms.

The unique mosaic of characters related to tooth replacements and the middle ear of eleutherodonts adds to growing evidence of complex transformations of mammalian characteristics. Their complex dentitions and occlusal patterns are probably adapted for omnivory and herbivory, showing that the volant and herbivorous lifestyle, previously known only in therian gliders, was also part of mammaliaform evolutionary experimentation during the Jurassic (Fig. 2 and Extended Data Fig. 7).

Online Content Methods, along with any additional Extended Data display items and Source Data, are available in the online version of the paper; references unique to these sections appear only in the online paper.

Data Availability All specimens of this study have been deposited at the Beijing Museum of Natural History. Graphics and phylogenetics data are provided in the Supplementary Information. Life Science Identifier (LSID): the new genus and species are registered with Zoobank (http://zoobank.org): urn:lsid:zoobank.org:pub:10917E53-A185-48A5-8C53-A30C5D7474A5.

Received 23 October 2016; accepted 14 July 2017.
Published online 9 August 2017.

1. Rowe, T. B. Definition, diagnosis, and origin of Mammalia. *J. Vertebr. Paleontol.* **8,** 241–264 (1988).
2. Luo, Z.-X. Transformation and diversification in early mammal evolution. *Nature* **450,** 1011–1019 (2007).
3. Kermack, K. A. *et al.* New multituberculate-like teeth from the Middle Jurassic of England. *Acta Palaeontol. Pol.* **43,** 581–606 (1998).
4. Butler, P. M. Review of the early allotherian mammals. *Acta Palaeontol. Pol.* **45,** 317–342 (2000).
5. Jenkins, F. A. Jr, Gatesy, S. M., Shubin, N. H. & Amaral, W. W. Haramiyids and Triassic mammalian evolution. *Nature* **385,** 715–718 (1997).
6. Luo, Z.-X., Gatesy, S. M., Jenkins, F. A. Jr, Amaral, W. W. & Shubin, N. H. Mandibular and dental characteristics of Late Triassic mammaliaform *Haramiyavia* and their ramifications for basal mammal evolution. *Proc. Natl Acad. Sci. USA* **112,** E7101–E7109 (2015).
7. Martin, T. *et al.* Mammals from the Late Jurassic Qigu Formation in the southern Junggar Basin, Xinjiang, northwest China. *Palaeodiv. et Palaeoenviron.* **90,** 295–319 (2010).
8. Averianov, A. O., Lopatin, A. V. & Krasnolutskii, S. A. The first Haramiyid (Mammalia, Allotheria) from the Jurassic of Russia. *Dokl. Biol. Sci.* **437,** 103–106 (2011).
9. Zhou, C.-F., Wu, S., Martin, T. & Luo, Z.-X. A Jurassic mammaliaform and the earliest mammalian evolutionary adaptations. *Nature* **500,** 163–167 (2013).
10. Zheng, X., Bi, S., Wang, X. & Meng, J. A new arboreal haramiyid shows the diversity of crown mammals in the Jurassic period. *Nature* **500,** 199–202 (2013).
11. Bi, S., Wang, Y., Guan, J., Sheng, X. & Meng, J. Three new Jurassic euharamiyidan species reinforce early divergence of mammals. *Nature* **514,** 579–584 (2014).
12. Meng, J., Bi, S., Zheng, X. & Wang, X. Ear ossicle morphology of the Jurassic euharamiyidan *Arboroharamiya* and evolution of mammalian middle ear. *J. Morphol.* (2016).
13. Liao, H.-Y. *et al.* Micro-ornamentations on carapaces of *Euestheria hingyuanensis* (Crustaceaa: Spinificance) and its biostratigraphic significance. *Acta Palaeontologica Sin.* **53,** 201–216 (2014).
14. Luo, Z.-X. *et al.* Mammalian evolution. Evolutionary development in basal mammaliaforms as revealed by a docodontan. *Science* **347,** 760–764 (2015).
15. Meng Q.-J. *et al.* New gliding mammaliaforms from the Jurassic. *Nature* http://dx.doi.org/10.1038/nature23476 (2017).
16. Yuan, C.-X., Ji, Q., Meng, Q.-J., Tabrum, A. R. & Luo, Z.-X. Earliest evolution of multituberculate mammals revealed by a new Jurassic fossil. *Science* **341,** 779–783 (2013).
17. Luo, Z.–X. Developmental patterns in Mesozoic evolution of mammal ears. *Annu. Rev. Ecol. Evol. Syst.* **42,** 355–380 (2011).
18. Meng, J., Wang, Y. & Li, C. Transitional mammalian middle ear from a new Cretaceous Jehol eutriconodont. *Nature* **472,** 181–185 (2011).
19. Lazzari, V. *et al.* Occlusal pattern in paulchoffatiid multituberculates and the evolution of cusp morphology in mammaliamorphs with rodent-like dentitions. *J. Mamm. Evol.* **17,** 177–192 (2010).
20. Wilson, G. P. *et al.* Adaptive radiation of multituberculate mammals before the extinction of dinosaurs. *Nature* **483,** 457–460 (2012).
21. Thorington R. W. Jr *et al.* The difficulties of identifying flying squirrels (Sciuridae: Pteromyini) in the fossil record. *J. Vertebr. Paleontol.* **25,** 950–961 (2005).
22. Jackson, S. M. & Schouten, P. *Gliding Mammals of the World* (CSIRO Publishing, 2012).
23. Meng, Q.-J. *et al.* Mammalian evolution. An arboreal docodont from the Jurassic and mammaliaform ecological diversification. *Science* **347,** 764–768 (2015).
24. Labandeira, C. C. The pollination of mid Mesozoic seed plants and the early history of long-proboscid insects. *Ann. Mo. Bot. Gard.* **97,** 469–513 (2010).
25. Radinsky, L. B. A new approach to mammalian cranial analysis, illustrated by examples of prosimian primates. *J. Morphol.* **124,** 167–180 (1968).
26. Santana, S. E. *et al.* The better to eat you with: functional correlates of tooth structure in bats. *Funct. Ecol.* **25,** 839–847 (2011).
27. Luo, Z.-X., *et al.* Evolution of dental replacement in mammals. *Carnegie Mus. Nat. Hist. Bull.* **36,** 159–175 (2004).
28. Anders, U. *et al.* Generalized individual dental age stages for fossil and extant placental mammals. *Paläontol. Zeitschr.* **85,** 321–339 (2011).
29. O'Meara, R. N. & Asher, R. J. The evolution of growth patterns in mammalian versus nonmammalian cynodonts. *Paleobiology* **42,** 439–464 (2016).
30. Sues, H.-D. The skull and dentition of two tritylodontid synapsids from the Lower Jurassic of western North America. *Bull. Mus. Comp. Zool.* **151,** 217–268 (1986).

Supplementary Information is available in the online version of the paper.

Acknowledgements We thank A. Shinya for fossil preparation; S. Bi, S. Gatesy, L. Heaney, H.-J. Li, Z.-J. Gao, T. Martin, B. Patterson, N. Shubin, X.-T. Zheng and C.-F. Zhou for access to comparative specimens. Funding supported Q.-J.M. (Beijing Scientific Commission) and Z.-X.L. (UChicago-BSD). Full acknowledgments are provided in the Supplementary Information.

Author Contributions Q.-J.M. and Z.-X.L. conceived the project; Q.-J.M., Y.-G.Z., D.L. and Q.J. acquired fossils and studied stratigraphy; all authors were involved in lab fossil work and interpretation; Z.-X.L. and D.M.G. did phylogenetic analyses; A.I.N. scanned and prepared graphics of fossils; Z.-X.L. composed figures; Z.-X.L., Q.-J.M. and D.M.G. led the writing, with feedback from all authors.

Author Information Reprints and permissions information is available at www.nature.com/reprints. The authors declare no competing financial interests. Readers are welcome to comment on the online version of the paper. Publisher's note: Springer Nature remains neutral with regard to jurisdictional claims in published maps and institutional affiliations. Correspondence and requests for materials should be addressed to Q.-J.M. (mengqingjin18@163.com), or Z.-X.L. (zxluo@uchicago.edu).

Reviewer Information *Nature* thanks G. Rougier and the other anonymous reviewer(s) for their contribution to the peer review of this work.

© 2017 Macmillan Publishers Limited, part of Springer Nature. All rights reserved.

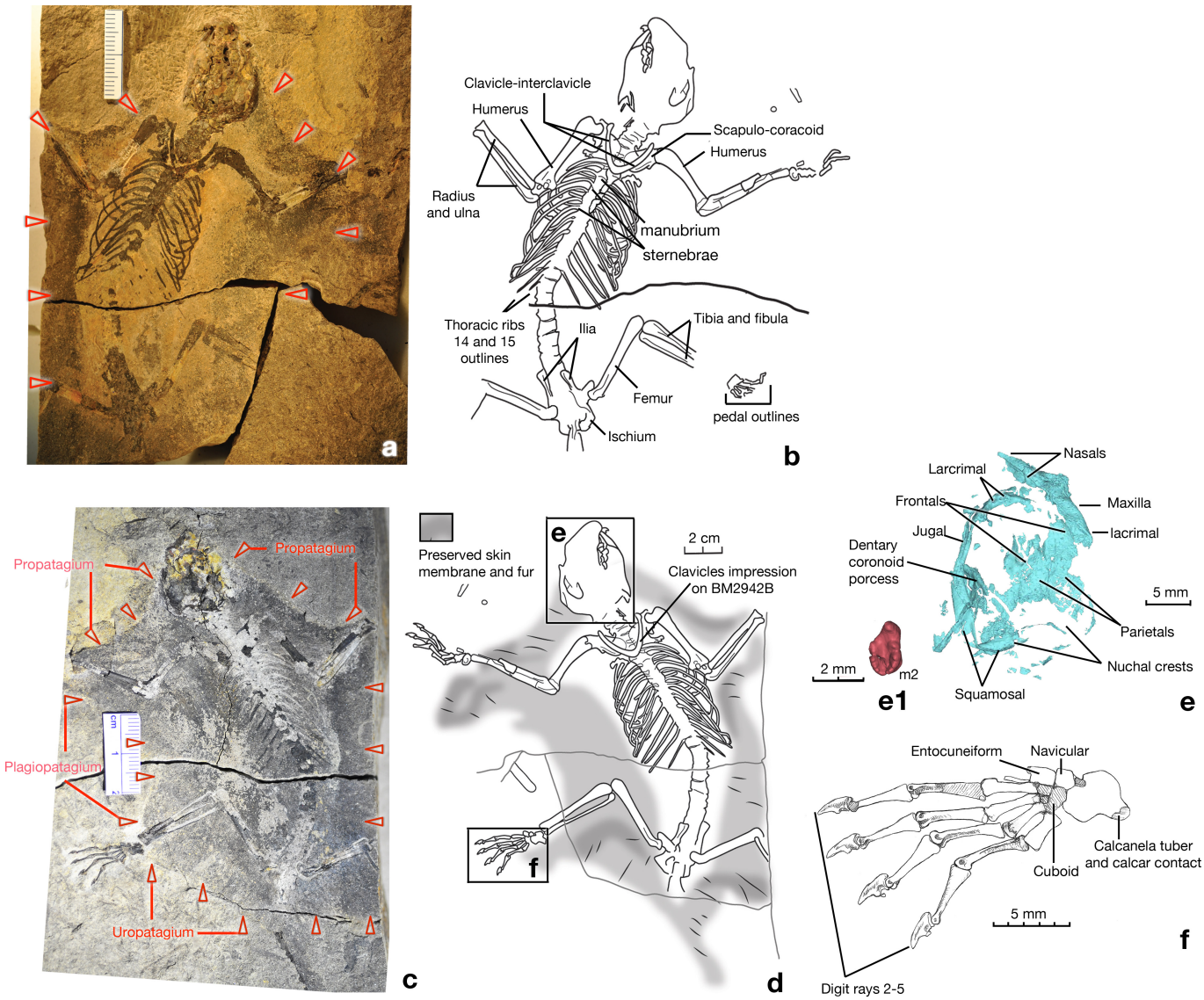

Extended Data Fig. 1. nature23483 (Nature Ms 2016-10-14701) ED Fig 1 replacement
(mengqingjin18@163.com; zxluo@uchicago.edu) 30 July 2017

Extended Data Figure 1 | Mammaliaform *Vilevolodon diplomylos* (Haramiyida, Eleutherodontidae) holotype (Beijing Museum of Natural History PM002942). a, **b**, BMNH2942A (main slab). Skeletal feature identification, and the outline of the carbonized patagial skin membranes (indicated by red arrows). **c**, **d**, BMNH2942B (counterpart). The outline of the carbonized patagial membranes: propatagium, plagiopatagium and uropatagium (indicated by red arrows), and their anatomical relationship to skeleton. **e**, Partial cranial roof and facial bones preserved on BMNH2942B, extracted by computed tomography (CT) scans and 3D rendering. **e1**, M_2 from counterpart BMNH2942B, in occlusal view. **f**, Right pes preserved on counterpart, with ventral view of tarsals and approximately lateral views of digit long bones (metatarsal 1 and digit 1 phalanges are not preserved).

© 2017 Macmillan Publishers Limited, part of Springer Nature. All rights reserved.

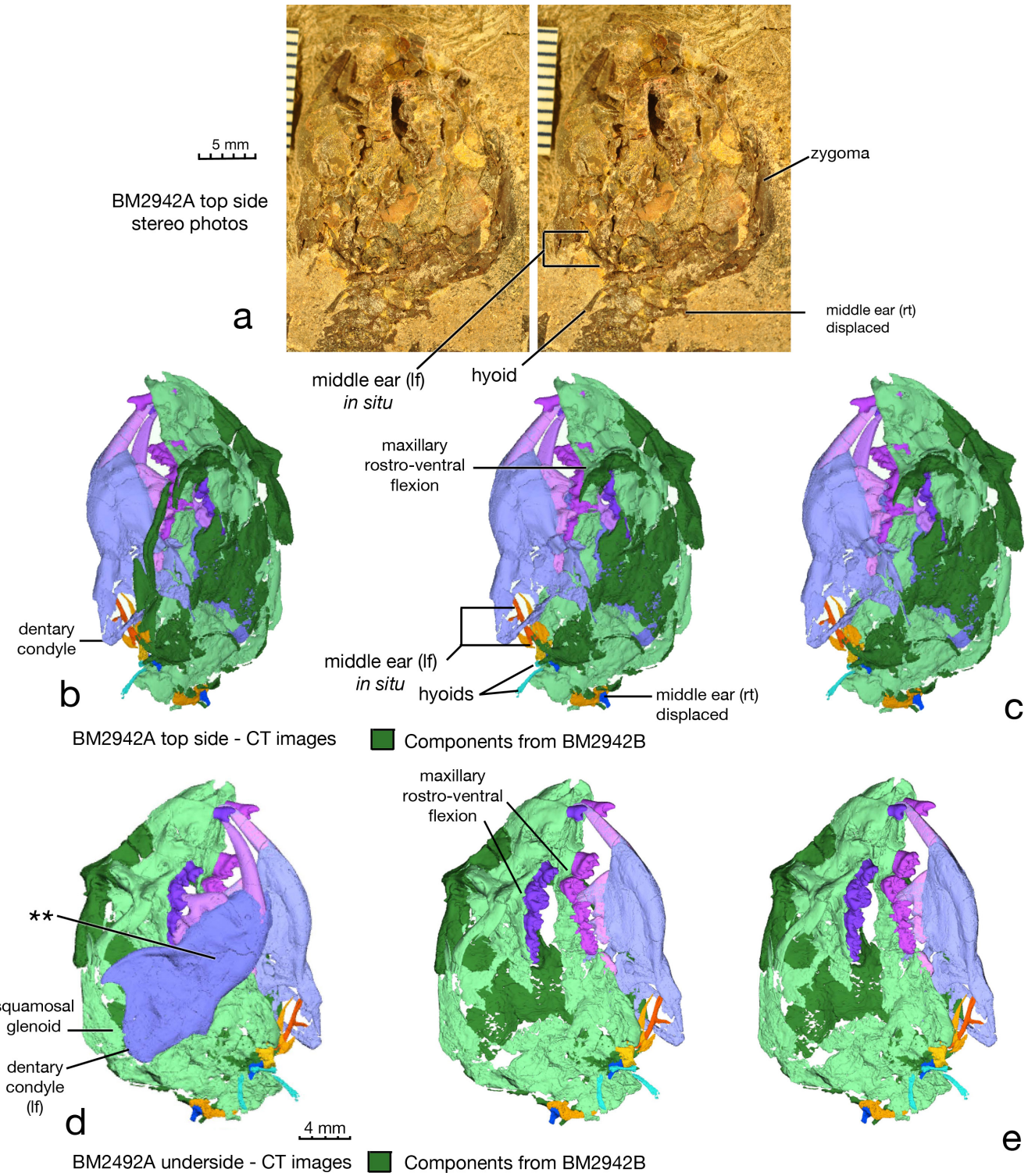

Extended Data Figure 2 | *Vilevolodon* skull on holotype main part (BMNH2942A). a, Stereo pair photographs of skull structures after preliminary preparation. **b**–**e**, CT scan rendering of BMNH2942A, viewed from the partially exposed top side of the skull. Dark green indicates bones segmented from counterpart BMNH2942B. **b**, Intact left zygoma. **c**, Stereo images of the skull with left zygoma removed to show the rostroventral flexion of maxillary and the premolar–molar row. **d**, Unexposed underside of the skull of BMN2942A visualized by CT segmentation, with right mandible in place. **e**, Stereo images of the skull with right mandible removed to show rostroventral flexion of right maxillary and its tooth row. ** indicates the irregular depression on the mandible formed by underlying massive tooth roots; but it is not a muscle fossa. Detailed analysis of the ear is provided in Extended Data Fig. 8, and comparative morphology in Extended Data Figs 8 and 9.

© 2017 Macmillan Publishers Limited, part of Springer Nature. All rights reserved.

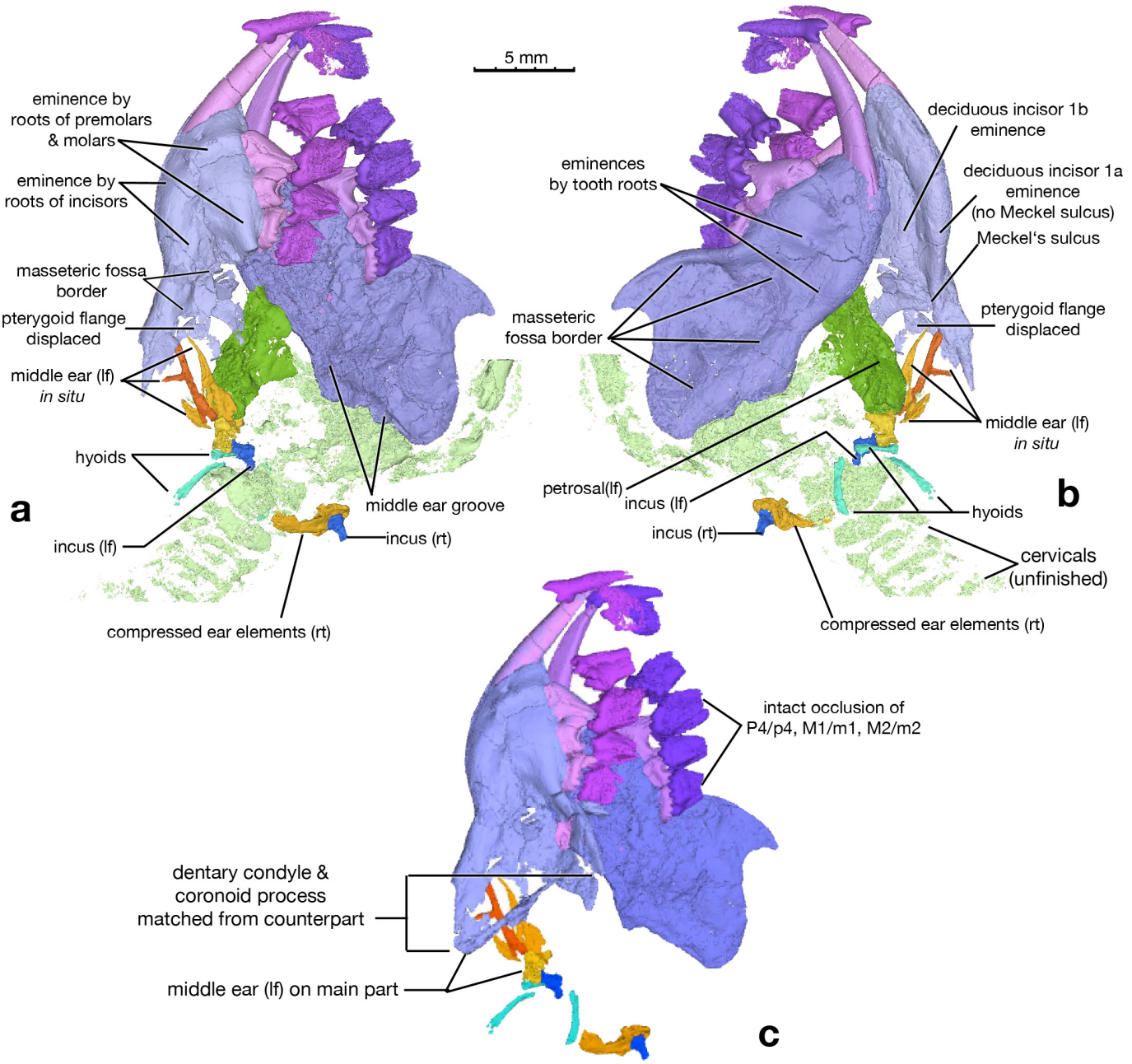

Extended Data Figure 3 | *Vilevolodon* mandible and teeth on holotype main part (BMNH2942A). Skull bones removed to expose the roots of upper teeth. **a**, CT scan rendering of BMNH2942A, viewed from the partially exposed top side of the skull; the intact occlusion of right upper and lower molars. Left dentary condyle and coronoid were preserved on the counterpart, helping to expose the full middle ear. **b**, CT rendering of the unexposed underside of the skull. **c**, Top side of the skull of BMNH2942A. The left mandible composite from the coronoid process and dentary condyle segmented from CT scans of the BMNH2942B counterpart. The left petrosal, the occipital and cervicals rendered invisible to highlight the relationship of middle ear to the mandible.

© 2017 Macmillan Publishers Limited, part of Springer Nature. All rights reserved.

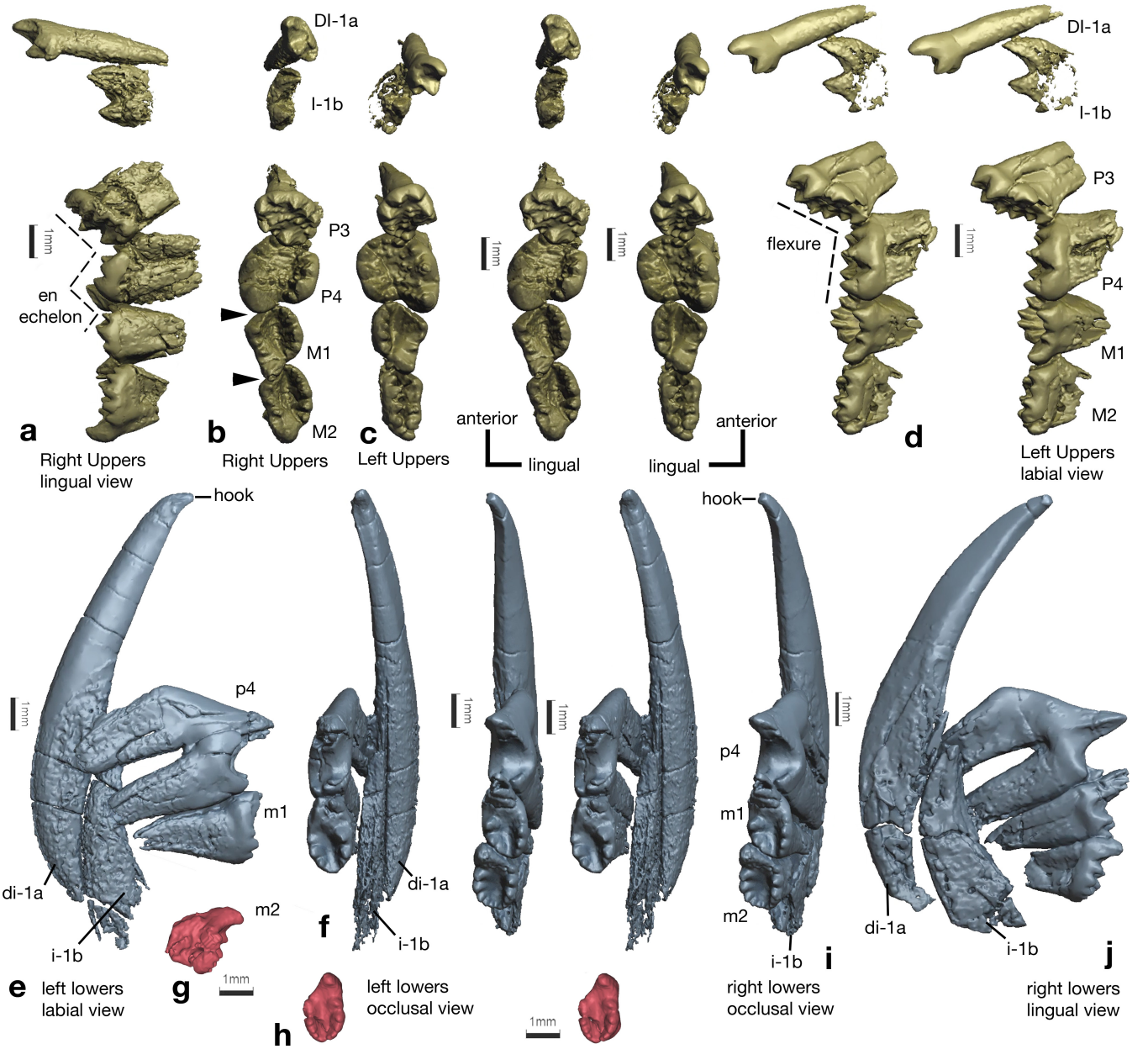

Extended Data Figure 4 | *Vilevolodon* dentition. a, Right upper teeth in lingual view. The dashed line shows the *en echelon* or step-wise pattern occlusal surfaces along the upper tooth row, a plesiomorphy of haramiyidans. **b**, Right upper teeth in ventral view (stereo pair photographs) with black arrows indicating successive lingual imbrication of M^1 and M^2. **c**, Left upper teeth (stereo pair photos). Note that M^2 was compressed in fossilization. **d**, Left upper teeth in labial view (stereo pair photos). The dashed line indicates P^3–P^4 flexure. **e**, Exposed left lower teeth: first generation deciduous lower incisor 1 (di-1a), second generation deciduous incisor 1 (i-1b), ultimate premolar P_4 and M_1 extracted from BMNH2942A. The M_2 was extracted from BMNH2942B. **f**, Left lower teeth (stereo pair photos) in occlusal view. Note the roots of deciduous incisors are entirely medial to roots of premolar or molars. The M_2 was extracted from BMNH2942B, and all other teeth are from BMNH2942A. **g**, Right lower M_2 from BMNH2942B. **h**, Right lower M_2 (stereo images, occlusal view). **i**, Right lower teeth (stereo images) in occlusal view from BMNH2942A. **j**, Right lower teeth in medial view. Bones removed digitally to expose tooth roots and the unerupted replacing incisors, highlighting the prolonged replacement of incisors relative to the adult premolars and molars.

© 2017 Macmillan Publishers Limited, part of Springer Nature. All rights reserved.

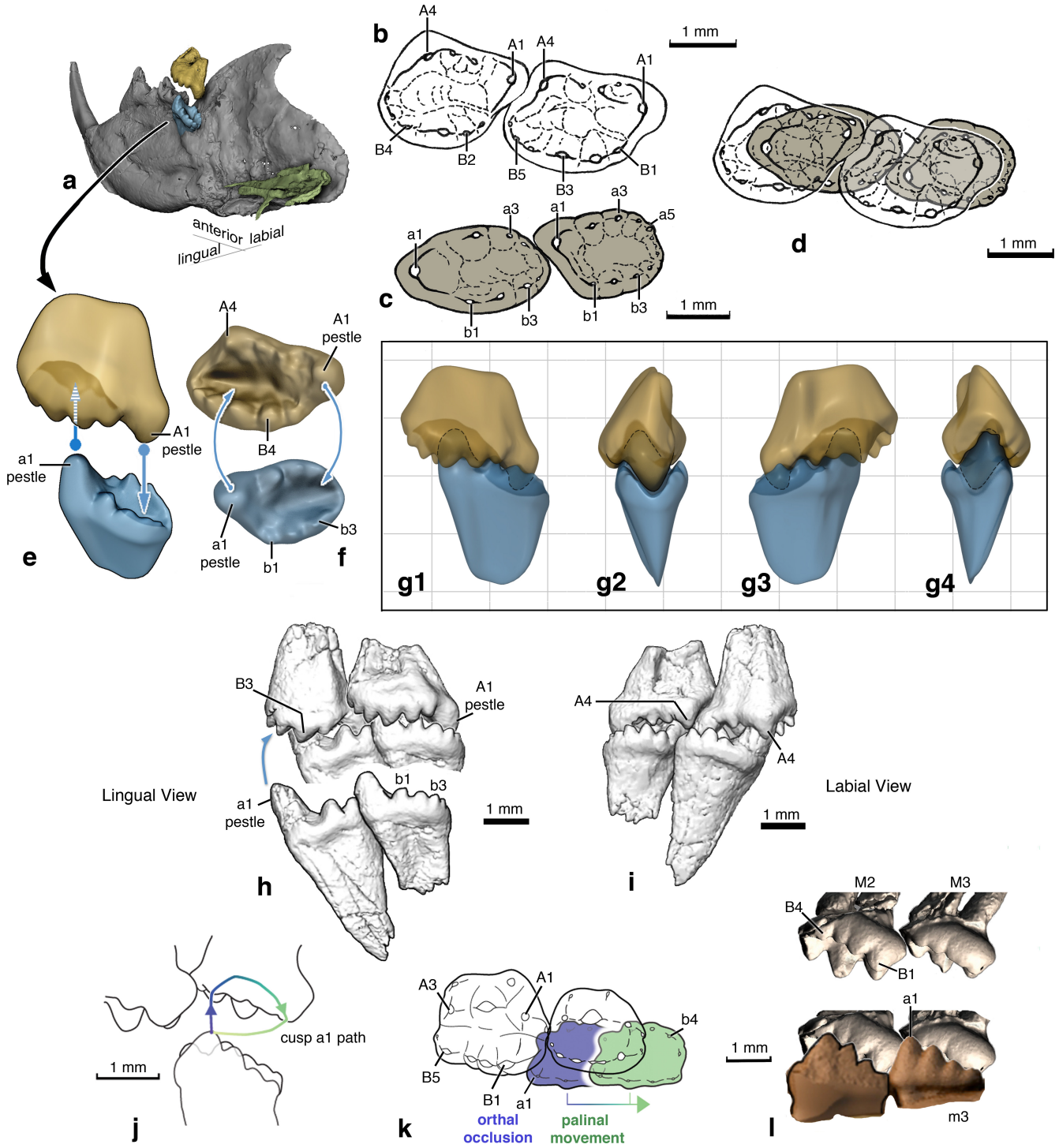

Extended Data Figure 5 | Dual mortar–pestle occlusion of *Vilevolodon* molars, in contrast to embrasure occlusion of *Haramiyavia*. **a**, *Vilevolodon* right mandible in oblique posterior view, highlighting the M^2/M_2 orientation and the attachment of the mandibular middle ear. **b**, Cusp pattern of upper molars (in translucent outline). Note that M^2 is imbricated more lingually to M^1. **c**, Cusp pattern of lower molars. Note that M_2 is imbricated more lingually to M_1, mirroring the imbrication of upper M^2 to M^1. **d**, Superimposition of upper M^1–M^2 (translucent outline) over lower M_1–M_2 (grey) for dual mortar–pestle occlusion of the upper and lower molars (see also Fig. 3). **e**, Oblique posterior view of right M^2 and M_2 in dual mortar–pestle occlusion: A_1 cusp (A_1 pestle) entering the M^2 basin and the A^1 cusp (A^1 pestle) entering the M_2 basin. **f**, Dual mortar–pestle occlusion of left M^2 and M_2 (solid surface models) in occlusal views. **g**, Dual mortar–pestle occlusion of right M^2 and M_2 surface models in medial (lingual) view (**g1**), posterior (distal) view (**g2**), lateral (labial) view (**g3**), and anterior (mesial) view (**g4**). **h**, Occlusion of right lower M_1–M_2 to right upper M^1–M^2 in lingual view, based on the best fit of opposing teeth. Note that the B^4–B^3 cusps of upper molars are always lingual to the lower lingual cusp row, but the B^1 cusp is always labial to lower lingual cusp row and in the lower median furrow. **i**, Occlusion of right M_1–M_2 to right M^1–M^2 in labial view. Note that cusp A^4 of the upper molar is always labial (lateral) to cusp A_1 of the lower molar. The upper labial row A^1–A^4 occludes obliquely over lower labial row B_1–B_4. There is no longitudinal alignment of cusp rows between the opposite upper and lower teeth, as in *Thomasia*, *Haramiyavia* and *Maiopatagium* (Fig. 3). **j**, Haramiyidan *Haramiyavia* occlusal trajectory (blue, orthal occlusion; green, palinal movement). **k**, *Haramiyavia*: transition of orthal phase (blue) to palinal phase (green) occlusion. Cusp row A_1–A_4 of the lower molar is lingual to cusp row B^1–B^5 of the upper molars. **l**, *Haramiyavia*: full orthal occlusion of M_3 with A_1 cusp in embrasure between upper M^2–M^3, and cusp row A_1–A_4 lingual to cusps B^1–B^5.

© 2017 Macmillan Publishers Limited, part of Springer Nature. All rights reserved.

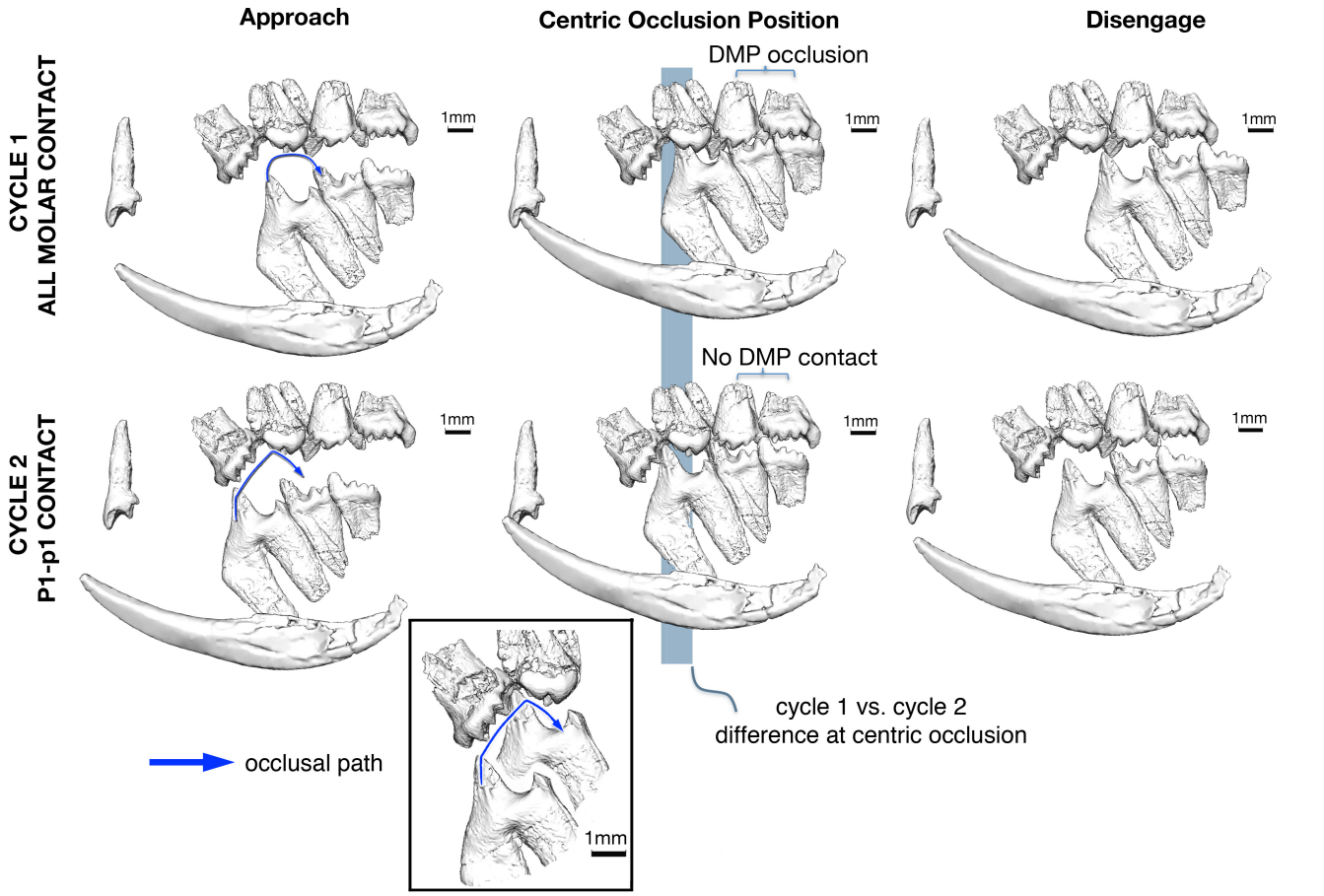

Extended Data Figure 6 | Autapomorphic occlusal features of *Vilevolodon*, including two inferred cycles of the molar occlusal movement. The upper tooth row has four teeth and is longer than the lower tooth row of three teeth. The upper P^3–P^4 flexure forms a prominent angle of the occlusal planes between the two premolars. In cycle 1 when lower M_1–M_2 is able to make full contact with M^1–M^2, P_4 and P^3 have no contact. In cycle 2, P_4/P^3 can make full contact, and their occlusion occurs only during cycle 2. But during this cycle, when the primary cusp of the P_4 makes full occlusal contact with P^3, the lower M_1 and M_2 can only barely contact the upper M^1 and M^2 and cannot make full contact. Occlusal movement was simulated by animation of STL models (see Supplementary Video 1) and inferred by maximal fit of upper and lower tooth occlusal surfaces. Blue arrows indicate the path of cusp A_1 of the lower premolar. The blue band in the central column shows the differences in the position of maximum intercuspation (centric occlusion of the P_4 primary cusp) between cycle 1 (above) and cycle 2 (below).

© 2017 Macmillan Publishers Limited, part of Springer Nature. All rights reserved.

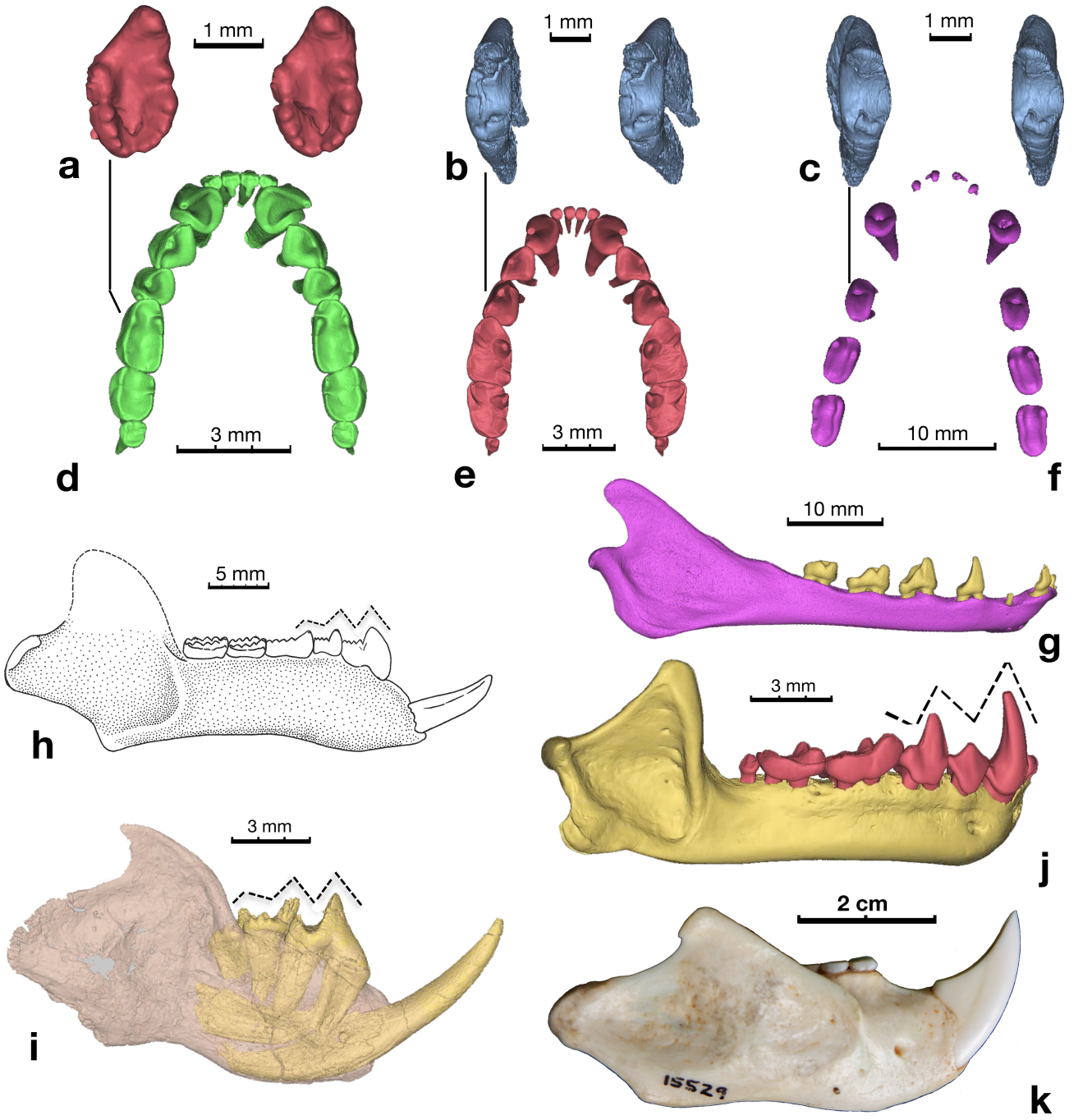

Extended Data Figure 7 | Dental and mandibular morphologies of eleutherodontids and extant frugivorous bats *Sturnira* and *Artibeus* (Chiroptera, Phyllostomidae), *Hypsignathus* (Megachiroptera: Pteropodidae), and frugivorous/omnivorous primate *Daubentonia*. **a**–**c**, *Vilevolodon* left M_2 (**a**) and left P_4 (**b**, **c**). **d**–**f**, Lower teeth of frugivorous bats: *Sturnira lilium lilium* (FMNH105870) (**d**); *Artibeus jamaicensis* (FMNH30776) (**e**); and *Hypsignathus monstrosus* (University of Chicago Biological Sciences Division Teaching Collection) (**f**). **g**, *Megaconus* right mandible in lateral view, highlighting the zigzag tooth row profile[9]. **h**, *Vilevolodon* right mandible in lateral view, highlighting the zigzag tooth row profile. **i**, *Hypsignathus* mandible in lateral view. **j**, *Artibeus* mandible in lateral view, highlighting the zigzag tooth row profile. **k**, Primate *Daubentonia* (FMNH15529) right mandible in lateral view. **a**, **d**–**f**, Similarities of lower molars of *Vilevolodon* with the basined lower molar talonids of frugivorous bats *Artibeus*, *Sturnira* and *Hypsignathus*. Eleutherodontids are particularly similar to the highly creased talonid basins of *Artibeus*, whereas *Maiopatagium* is more similar to *Sturnira* and pteropodid bats in molar pattern. **b**–**e**, **f**, Similarities of lower premolar of *Vilevolodon* to those of *Sturnira* and *Hypsignathus*. **g**, **h**, Similarity of the zigzag tooth row profile of lower premolars and molars of *Megaconus* and eleutherodontids to those of frugivorous bats. **g**, **h**, **k**, Similarity in mandibles of eleutherodonts and the primate *Daubentonia* (FMNH15529), which is frugivorous and insectivorous.

© 2017 Macmillan Publishers Limited, part of Springer Nature. All rights reserved.

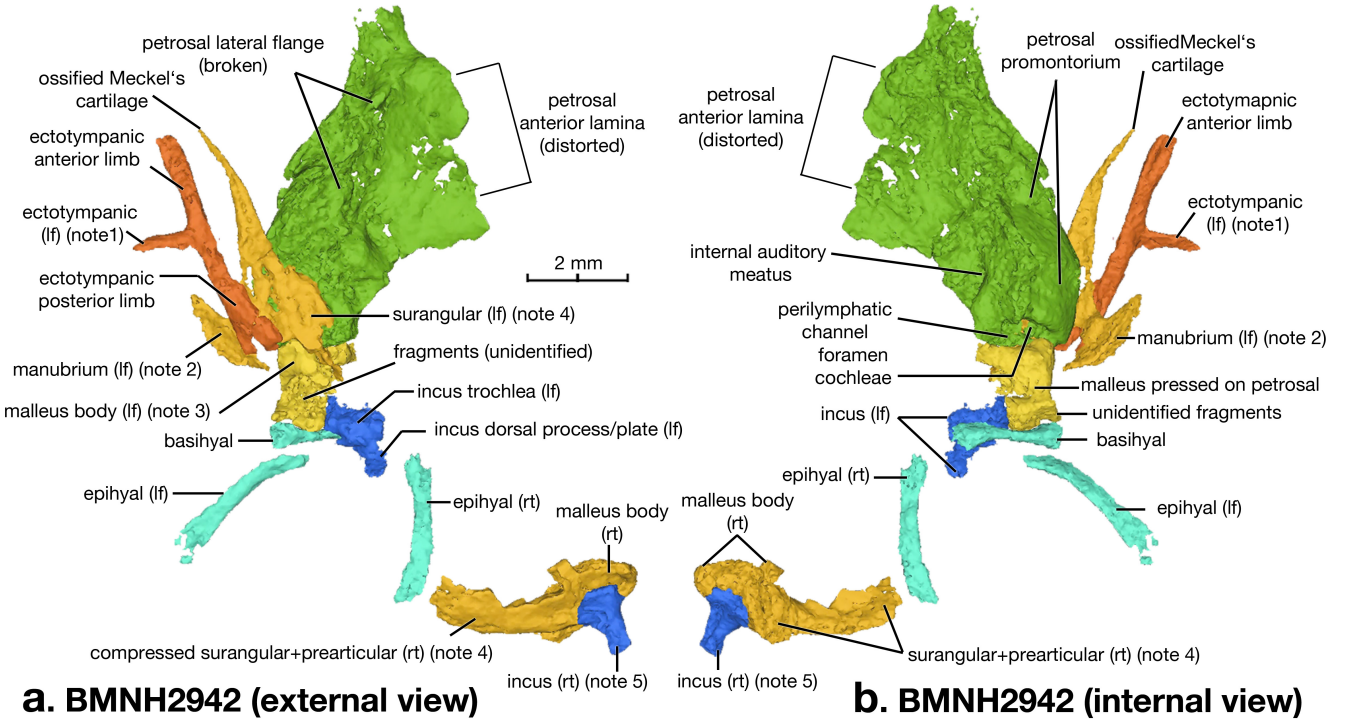

Extended Data Figure 8 | *Vilevolodon* middle ear structure preserved in holotype (BMNH2942) and interpretive reconstruction. **a**, BMNH2942A in approximately ventral view. External and exposed aspect of left petrosal (partial) and middle ear bones as preserved. The dentary and cervical vertebrae are digitally removed so that the view of the middle ear features is unobstructed. **b**, BMNH2942A 'internal' view (underside of the fossil in matrix), showing the petrosal (partially segmented) and middle ear bones. **c**, Interpretative reconstruction of the middle ear bones of *Vilevolodon*, based on middle ear bones exposed in CT scans and 3D segmentation. **d**, A composite reconstruction of the middle ear of eutriconodonts. **e**, Cynodont *Kayentatherium* (redrawn from ref. 30). **f**, Pre-mammaliaform cynodont *Cynognathus* middle ear (redrawn from ref. 31) Note 1 to readers: the gracile ectotympanic (reflected lamina of angular), and this gracile and relatively straight morphology is similar to the reflected lamina of several non-mammalian cynodonts. The angle of attachment to the anterior–posterior limbs of ectotympanic (homologue of the angular) is slightly distorted by fossilization. Notes 2 and 3 to readers: the manubrial portion of the malleus (Note 2) is partly attached to the malleus body (Note 3), but there is a gap between these two structures owing to imperfect preservation. Note 4: the posterior end of Meckel's cartilage is attached to a large sliver of bone. The latter is tentatively interpreted to be a surangular, which in non-mammalian cynodonts is typically parallel to the gonial part (the prearticular) of the malleus (although separated from the latter). There appears to be a suture between the prearticular part of the malleus, and the putative surangular. We infer that the Meckel's cartilage and the ectotympanic, as preserved in close association, contact each other loosely. But they became slightly separated from each other during fossilization. We reconstructed these two elements as contiguous, as in cynodonts and other mammaliaforms, as demonstrated in **c**.

31. Kermack, K. A., Mussett, F. & Rigney, H. W. The lower jaw of *Morganucodon*. *Zool. J. Linn. Soc.* **53,** 87–175 (1973).

© 2017 Macmillan Publishers Limited, part of Springer Nature. All rights reserved.

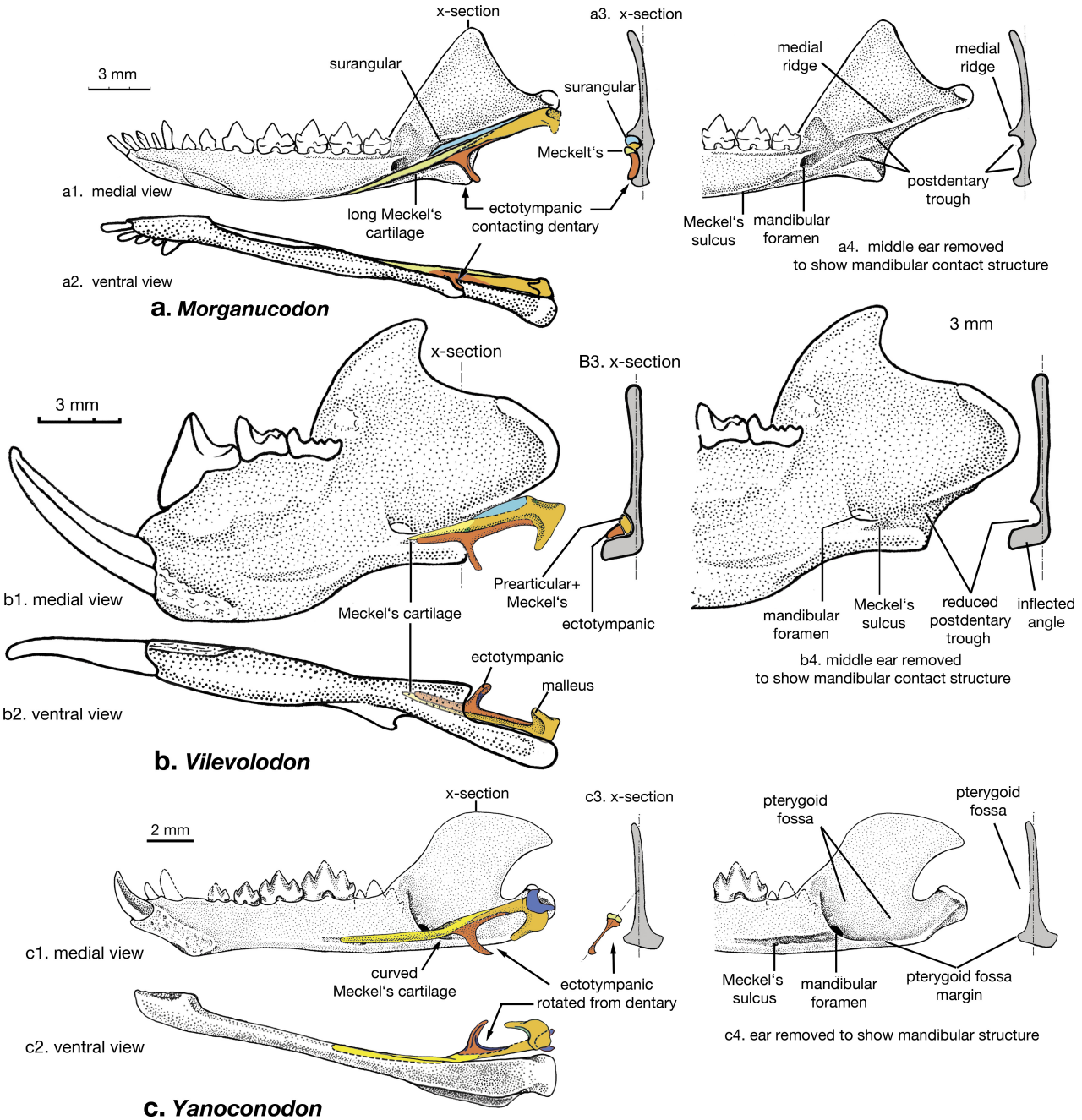

Extended Data Figure 9 | Comparative morphology of the mandibles and partial mammalian middle ears of extinct Mesozoic mammaliaforms. a, *Morganucodon* and several mammaliaforms possess plesiomorphic mandibular middle ear of cynodonts (MMEC). The ectotympanic (homologue of the angular) is nestled in the angular concavity of the mandible. The surangular and the gonial part (homologue of the prearticular) of the malleus make full contact with a broad postdentary trough that extends posteriorly to near the dentary condyle under the medial ridge. The Meckel's element (ossified cartilage) starts from the postdentary trough, passes anteriorly below the mandibular foramen, and extends further anteriorly into a long Meckel's sulcus below the mandibular tooth row. **b**, Eleutherodontid *Vilevolodon* shows a mandibular connection of the middle ear, although much more reduced (antero-posteriorly shortened) than those of other mammaliaforms. The anterior limb of the ectotympanic and the gonial part (prearticular) of the malleus are nestled in a reduced postdentary trough on the internal aspect of the inflected mandibular angle. The groove occupies the identical position of the postdentary trough in the angular region of other mammaliaforms. However, it is narrower and much shorter than the postdentary trough of other mammaliaforms. The trough is shorter (an apomorphic trait) and does not extend posteriorly to the dentary condyle, in contrast to the postdentary trough in other mammaliaforms. The short and tapering Meckel's cartilage ends below the mandibular foramen, but it does not extend further anteriorly to the mandibular body below the tooth row. The Meckel's element and its corresponding Meckel's sulcus are much shorter than those of other mammaliaforms, eutriconodonts and spalacotherioids. The gonial portion of the malleus (and the putative surangular) also contacts the ventral margin of the mandible. We infer that, in *Vilevolodon*, the ectotympanic (retroarticular process) and the manubrial part of the malleus are rotated medially and horizontally, away from the mandible (**b3**), as in eutriconodonts. **c**, Eutriconodont *Yanoconodon*, highlighting the massive ossified Meckel's cartilage that connects the middle ear to the mandible. Owing to the curvature and mid-length bending of Meckel's element, the ectotympanic and malleal manubrium rotated medially and away from the mandible[32].

32. Luo, Z.-X., Chen, P., Li, G. & Chen, M. A new eutriconodont mammal and evolutionary development in early mammals. *Nature* **446,** 288–293 (2007).

© 2017 Macmillan Publishers Limited, part of Springer Nature. All rights reserved.

nature research

Corresponding author(s): Zhe-Xi Luo

☐ Initial submission ☐ Revised version ☒ Final submission

Life Sciences Reporting Summary

Nature Research wishes to improve the reproducibility of the work that we publish. This form is intended for publication with all accepted life science papers and provides structure for consistency and transparency in reporting. Every life science submission will use this form; some list items might not apply to an individual manuscript, but all fields must be completed for clarity.

For further information on the points included in this form, see Reporting Life Sciences Research. For further information on Nature Research policies, including our data availability policy, see Authors & Referees and the Editorial Policy Checklist.

Experimental design

1. Sample size

Describe how sample size was determined.

Our study reports on finding of original fossils. All fossil specimens available for this study has been have been reported. Their skeletal and dental measurements of the single holotype specimens and comparative measurements of skeletons of extant mammals are reported in supplementary information. Skeletal and dental measurement of the single holotype specimen of the new fossil species are reported in SI Tables S1 and S2.

2. Data exclusions

Describe any data exclusions.

No data on fossils available for this study have been excluded. All extant specimens for morphological comparison are also figured in the study. The phylogenetic analysis presented in our study is one of the largest ever on mammaliaforms. To the best of our ability, we exhausted all character sampling.

3. Replication

Describe whether the experimental findings were reliably reproduced.

Phylogenetic analyses were performed in both maximum parsimony analysis and Bayesian analyses. These two alternative analyses produced the same placement of our clade (haramiyidans) on mammaliaform evolutionary tree.

4. Randomization

Describe how samples/organisms/participants were allocated into experimental groups.

Not applicable

5. Blinding

Describe whether the investigators were blinded to group allocation during data collection and/or analysis.

Not applicable

Note: all studies involving animals and/or human research participants must disclose whether blinding and randomization were used.

6. Statistical parameters

For all figures and tables that use statistical methods, confirm that the following items are present in relevant figure legends (or in the Methods section if additional space is needed).

n/a	Confirmed
☐	☒ The exact sample size (*n*) for each experimental group/condition, given as a discrete number and unit of measurement (animals, litters, cultures, etc.)
☒	☐ A description of how samples were collected, noting whether measurements were taken from distinct samples or whether the same sample was measured repeatedly
☒	☐ A statement indicating how many times each experiment was replicated
☒	☐ The statistical test(s) used and whether they are one- or two-sided (note: only common tests should be described solely by name; more complex techniques should be described in the Methods section)
☒	☐ A description of any assumptions or corrections, such as an adjustment for multiple comparisons
☒	☐ The test results (e.g. *P* values) given as exact values whenever possible and with confidence intervals noted
☒	☐ A clear description of statistics including central tendency (e.g. median, mean) and variation (e.g. standard deviation, interquartile range)
☒	☐ Clearly defined error bars

See the web collection on statistics for biologists for further resources and guidance.

Software

Policy information about availability of computer code

7. Software

Describe the software used to analyze the data in this study.	Not applicable

For manuscripts utilizing custom algorithms or software that are central to the paper but not yet described in the published literature, software must be made available to editors and reviewers upon request. We strongly encourage code deposition in a community repository (e.g. GitHub). *Nature Methods* guidance for providing algorithms and software for publication provides further information on this topic.

Materials and reagents

Policy information about availability of materials

8. Materials availability

Indicate whether there are restrictions on availability of unique materials or if these materials are only available for distribution by a for-profit company.	The phylogenetic matrix and the character list that are the basis of the main evolutionary hypothesis is already presented in Supplementary Information. The STL files on the teeth and jaws from the CT scanning of the type specimen will be deposited in MorphoSource.Org, a public repository of CT-derived data. Because we are still working on the petrosal (the inner ear), and cervical vertebral column and the rest of the skull structure from the master CT dataset, we cannot yet release the raw CT dataset that is under active study for other structures, which cannot be covered by short Nature paper.

9. Antibodies

Describe the antibodies used and how they were validated for use in the system under study (i.e. assay and species).	Not applicable

10. Eukaryotic cell lines

a. State the source of each eukaryotic cell line used.	Not applicable
b. Describe the method of cell line authentication used.	Not applicable
c. Report whether the cell lines were tested for mycoplasma contamination.	Not applicable
d. If any of the cell lines used are listed in the database of commonly misidentified cell lines maintained by ICLAC, provide a scientific rationale for their use.	Not applicable

Animals and human research participants

Policy information about studies involving animals; when reporting animal research, follow the ARRIVE guidelines

11. Description of research animals

Provide details on animals and/or animal-derived materials used in the study.	Not applicable

Policy information about studies involving human research participants

12. Description of human research participants

Describe the covariate-relevant population characteristics of the human research participants.	Not applicable